KERNFORSCHUNGSZENTRUM

KARLSRUHE

Juni 1968

KFK 786
EUR 3958 e

Institut für Neutronenphysik und Reaktortechnik

Reactor Dynamics Topics Recently Investigated at Karlsruhe

H. Borgwaldt, H. Küsters, G. Kußmaul, H. Meister, K. Thurnay

GESELLSCHAFT FÜR KERNFORSCHUNG M. B. H.

KARLSRUHE

K E R N F O R S C H U N G S Z E N T R U M
K A R L S R U H E

Juni 1968

KFK- 786
EUR- 3958 e

Institut für Neutronenphysik und Reaktortechnik

Reactor Dynamics Topics Recently Investigated at Karlsruhe*)+)

by

H. Borgwaldt, H. Küsters, G. Kussmaul, H. Meister, K. Thurnay

*) Paper presented to the meeting on "Industrial Needs and Academic Research in Reactor Kinetics", Brookhaven National Laboratory, April 8-9, 1968.

+) Work performed within the association in the field of fast reactors between the European Atomic Energy Community (Euratom) and Gesellschaft für Kernforschung m.b.H., Karlsruhe.

GESELLSCHAFT FÜR KERNFORSCHUNG MBH. KARLSRUHE

Abstract

In a review of recent work at Karlsruhe results from three fields of investigations are reported:

(1) The theory of neutron noise in a reactor with prompt and delayed neutrons was extended to include an external control loop.

(2) For two weakly, symmetrically coupled cores, with equal generation times and delayed neutron parameters, the kinetics equations for a step change in reactivity could be solved in terms of familiar point-reactor expressions. Measurements on a two-slab Argonaut reactor confirmed the model and were used to determine reactivity and coupling coefficients.

(3) The analysis of fast reactor dynamics with digital and analog computing methods has been improved, especially for steam cooled systems including the primary circuit. Several coolant channels can be treated in parallel with appropriate equations of state for the coolant. - In large power excursions with core disassembly the autocatalytic effect in two-zoned cylindrical reactors is discussed in detail, showing the inadequacy of the normally used theoretical model.

1. Neutron noise in a reactor with feedback.

The theory of neutron fluctuations in reactors |1| was extended to include the influence of an external control loop |2|. The results can be used to compute fluctuations occurring in critical zero-power assemblies during long-time, automatically controlled experiments. Also, they aid in understanding the role of feedback in power reactor noise.

In fig. 1 the reactor is perturbed by an uncorrelated reactivity input $\rho_o(t)$ with zero average and a PSD (= power spectral density)

$$P_o(\omega) = \int_{-\infty}^{\infty} \langle \rho_o(t)\, \rho_o(t+\tau) \rangle \quad e^{-i\omega\tau}\, d\tau. \tag{1.1}$$

$\langle\ \rangle$ denotes an expectation value; here and in (1.15) this is also a time average.

$\rho = \rho_o - \rho_c$ is the net reactivity, and

$$\rho_c(t) = \int_{o}^{\infty} g(\theta)\, \frac{N(t-\theta)-N_o}{N_o}\, d\theta \tag{1.2}$$

is the control reactivity (feedback) with N = neutron population, N_o = constant demand value. As usual,

$$|N-N_o| \ll N_o \quad \text{and} \quad |\rho_o| \ll \beta \tag{1.3}$$

is postulated. For the Fourier-transform $G(\omega)$ of the controller response function $g(t)$ we assume a form

$$G(\omega) = \sum_{j=1}^{J} \frac{a_j}{i\omega - p_j} \quad (\mathrm{Re}\ p_j < 0). \tag{1.4}$$

In fig. 1 we have two neutron detectors of the absorber type, with sensitivities W_a and W_b (pulses/fission). We are interested in the PSD $S(\omega)$ of the noise in the signal of the detector outside the control loop. For $S(\omega)$ we derived an expression

$$S(\omega) = \sum_{k=1}^{4} S_k(\omega) \tag{1.5}$$

with the contributions

$$S_1(\omega) = W_b \; F \; r_b, \tag{1.6}$$

$$S_2(\omega) = W_b^2 \; F^2 \; P_o(\omega) \; |H(\omega)|^2, \tag{1.7}$$

$$S_3(\omega) = W_b^2 \; F \; \overline{(\nu(\nu-1)} \; / \; \bar{\nu}^2) \; |H(\omega)|^2, \tag{1.8}$$

$$S_4(\omega) = W_b^2 \; F \; (r_a/W_a) \; |G(\omega)|^2 \; |H(\omega)|^2. \tag{1.9}$$

$\overline{\nu(\nu-1)}/\bar{\nu}^2 \simeq .80$, F = mean fission rate, $H(\omega)$ = frequency response function of the reactor with feedback. In conventional notation

$$H(\omega) = H_o(\omega) \; / \; [1+G(\omega) \; H_o(\omega)], \tag{1.10}$$

$$H_o(\omega) = (1- \sum_{k=1}^{6} \frac{\beta_k i\omega}{\lambda_k+i\omega}) \; / \; (i\omega\ell+ \sum_{k=1}^{6} \frac{\beta_k i\omega}{\lambda_k+i\omega}). \tag{1.11}$$

For each detector, the parameter |3|

$$r = \langle\xi^2\rangle \; / \; \langle\xi\rangle^2 \geq 1 \tag{1.12}$$

is determined by the distribution of detector pulse amplitudes ξ.

The contribution S_1 is white detector noise. To obtain S_2 we regard approximately the system of reactor, control loop and detector as a linear element responding to the reactivity input $\rho_o(t)$. For such elements an often-used relation exists between the PSD's of input and output, which leads directly to (1.7), when the normalizations of S_1 and S_2 are made consistent.

Fission reactions, the dominant source of fluctuations in subcritical assemblies, can tentatively be treated as an independent driving reactivity with a white spectrum. When we insert $P_o'(\omega) = \text{const}$ into (1.7) to get S_3, we deduce the correct normalization versus S_1 by extrapolating $\omega \to \infty$. Then $H(\omega) \approx H_o(\omega)$ and the formulas for zero-power noise |3, 4| are applicable, yielding (1.8) for S_3.

The last source of noise to be considered are spurious detector signals in the control loop. If their overall PSD is $R_s(\omega)$, we will get a spurious feedback reactivity $\rho_s(t)$ with a PSD

$$P_s(\omega) = |G(\omega)|^2 R_s(\omega) / (W_a F)^2 \qquad (1.13)$$

The detector signal in the control loop is contaminated by white detector noise with

$$R_s(\omega) = \text{const} = W_a F r_a , \qquad (1.14)$$

cf. (1.6). When in the control loop no other sources of noise are present, we may insert (1.14) and (1.13) into (1.7) and obtain (1.9) for S_4.

In ref. 2 this partly phenomenological development is supplemented by a rigorous stochastic treatment, of which a few important features shall be reported.

The PSD $S(\omega)$ is defined as the Fourier-transform of the autocorrelation function $R_b(\tau)$ of the detector signal. For $\tau > o$

$$R_b(\tau) = W_b F r_b \delta(\tau) + W_b^2 \langle N(t) N^*(t,\tau) - N_o^2 \rangle / (\bar{\nu}\ell)^2 . \qquad (1.15)$$

δ = Dirac's function, $N(t)$ = expected number of neutron (unconditional) at time t, $N^*(t,\tau)$ = expected number of neutrons (conditional) at time $t+\tau > t$ <u>after</u> one detector pulse at time t. For $\tau < o$ this definition is supplemented by demanding symmetry,

$$R_b(\tau) = R_b(-\tau) . \qquad (1.16)$$

On account of (1.2) and (1.4) the feedback reactivity becomes a sum

$$\rho_c(t) = \sum_{j=1}^{J} \rho_j(t) \tag{1.17}$$

of partial contributions, which obey equations

$$\frac{d}{dt}\rho_j(t) = \frac{a_j}{W_a F} R(t) + p_j \rho_j(t) - a_j \tag{1.18}$$

$R(t) = W_a N(t)/(\bar{\nu}\ell)$ is for the control detector the expected pulse rate at time t. The actual behaviour of each term $\rho_j(t)$ is composed of step changes of an average amplitude $a_j/(W_a F)$ and of slow changes according to

$$\frac{d}{dt}\rho_j(t) = p_j \rho_j(t) - a_j \tag{1.19}$$

Let $p(n,\vec{c},\vec{\rho},t)$ be the probability density, at time t, for a state with n neutrons, $\vec{c} = (c_1,\ldots,c_6)$ for the precursor populations and $\vec{\rho} = (\rho_1,\ldots,\rho_J)$ for the state of the reactivity feedback. Define a generating function

$$f(u,\vec{v},\vec{x},t) = \sum_{(n,c_1,\ldots,c_6)} \cdots \sum u^n v_1^{c_1} \cdots v_6^{c_6} \times \tag{1.20}$$

$$\times \int\int \cdots \int \exp i(\rho_1 x_1 + \cdots + \rho_J x_J)\, p(n,\vec{c},\vec{\rho},t)\, d\rho_1 \cdots d\rho_J$$

with the obvious normalization

$$f(u=v_1=\cdots=v_6=1,\ \vec{x}=0,\ t) \equiv 1. \tag{1.21}$$

Expressions for $\partial p(n,\vec{c},\vec{\rho},t)/\partial t$ can be derived from elementary considerations taking into account transitions by (1) precursor decays, (2) fission, (3) neutron leakage or capture undetected by the control detector, (4) neutron detection by the control detector with a step change in each term ρ_j ($j = 1,\ldots,J$), (5) slow changes in the ρ_j's according to (1.19).

If no other perturbations in the feedback loop (e.g. electronic noise) are present, we get in terms of the generating function (1.20) an exact equation

$$\frac{\partial f}{\partial t} = \sum_{j=1}^{J} ix_j \left(p_j \frac{\partial f}{i\partial x_j} - a_j f\right) + \sum_{k=1}^{6} \lambda_k (u-v_k) \frac{\partial f}{\partial v_k}$$

$$+ \frac{1}{\ell} \frac{\partial f}{\partial u} \left[1-u+ \frac{1+\rho_o(t)}{\nu} (\psi(u,\vec{v})-1)\right. \tag{1.22}$$

$$\left. + \frac{W_a}{\nu} \left(\int_o^\infty w_a(\xi) \exp \sum_{j=1}^{J} \frac{ix_j a_j \xi}{W_a F<\xi>} d\xi - 1\right)\right]$$

$$- \frac{1}{\ell i} \sum_{j=1}^{J} \frac{\partial^2 f}{\partial u \partial x_j} (\psi(u,\vec{v})-1)$$

Herein $w_a(\xi)$ gives, for the control detector, the distribution of pulse amplitudes ξ.

$$\psi(u,\vec{v}) = \sum_{(m_o,..m_6)} \sum q(m_o,...,m_6)\, u^{m_o} v_1^{m_1}..v_6^{m_6} \tag{1.23}$$

is the probability generating function formed from the probabilities $q(m_o,..,m_6)$ to obtain in one fission m_o prompt neutrons, m_1 precursors of group 1 etc. Other symbols have been explained or are used conventionally.

We need two solutions of (1.22). The first, $f_o(u,\vec{v},\vec{x},t)$, must be free of all transients, in order to describe a controlled reactor responding to a reactivity perturbation $\rho_o(t)$, but otherwise stationary. For insertion into (1.15) one gets from f_o

$$N(t) = \frac{\partial f_o}{\partial u} (u=v_1=..=v_6=1,\ \vec{x}=o,\ t). \tag{1.24}$$

The second solution, $f^*(u,\vec{v},\vec{x},t;t_o)$, is defined for arbitrary t_o and all $t>t_o$ and describes the same reactor under the condition, that at t_o one neutron was detected. For (1.15) we, thus, get

$$N^*(t,\tau) = \frac{\partial f^*}{\partial u} (u=v_1=..=v_6=1,\ \vec{x}=o,\ t+\tau;\ t). \tag{1.25}$$

The actual neutron population n at t_o determines the probability of detecting a neutron at that time. Detection by the detector outside the control loop removes one neutron and leaves other parameters unchanged. These considerations, the normalization (1.21) and (1.24) impose an initial condition

$$f^{*}(u,\vec{v},\vec{x},t_o;t_o) = \frac{\partial f_o}{\partial u}(u,\vec{v},\vec{x},t_o)/N(t_o). \tag{1.26}$$

Unfortunately, the second order derivatives in (1.22), which describe feedback, make this equation almost untractable. Therefore, in ref. 2 two assumptions were made: (1) The demand value N_o is sufficienty high; (2) deviations of the actual neutron population n from N_o have small relative amplitude. Then, one may approximate

$$\frac{\partial^2 f}{\partial u \partial x_j} \approx N_o \frac{\partial f}{\partial x_j}. \tag{1.27}$$

After this substitution, we may, in principle, expand f near $u=v_1=..=v_6=1$, $\vec{x}=o$, and calculate from (1.22) recursively the time dependent expansion coefficients to the desired order. In practice, a labour-saving procedure can be used.

With N(t) and $N^{*}(t,\tau)$ computed in this way, the autocorrelation function (1.15) yielded after its Fourier-transformation an almost perfect verification of the formulas for $S(\omega)$ as given by (1.5) to (1.9). Only the term $S_3(\omega)$ had to be corrected by a factor, which can, however, be neglected in practice, as its maximum deviation from unity is $\approx \beta/2$.

In fast zero-power assemblies the assumptions leading to (1.27) are not always valid. But recent (unpublished) investigations have led to a verification of the formulas given under relaxed conditions, which are almost universally fulfilled: (1) High precursor populations, (2) slow changes in input and feedback reactivity, i.e. many prompt neutron chains elapse, before such changes become significant.

2. Kinetics and reactivity determination in a system of two loosely coupled cores.

Reactivity determinations in a reactor by observation of the time-behaviour of the neutron population, e.g. in pulsed neutron-, period- or rod drop-measurements, are mostly evaluated on the basis of the point reactor-model. In a system composed of two loosely coupled cores each core tends to behave independently. In the frame of the two-point reactor-model [5-8], we theoretically analyzed for a coupled two-core system the time-behaviour following step changes in reactivity. The main importance was laid on rod drop-measurements, where the time behaviour is predominantly determined by the delayed neutron precursors and the neutron transition time between core zones can be neglected [9]. The theoretical and experimental results [10] indicate that the reactivity and the coupling coefficients can be obtained from simple measurements.

Theory. In the case of equal prompt neutron generation times Λ and precursor parameters (β_i, λ_i) the kinetics equations for two coupled point reactors, A and B, are given as

$$\frac{d}{dt} n_X(t) = \frac{\rho_X(t) - \beta}{\Lambda} n_X(t) + \sum_{i=1}^{6} \lambda_i C_{Xi}(t) + \frac{\varepsilon_{YX}}{\Lambda} n_Y(t), \tag{2.1}$$

$$\frac{d}{dt} C_{Xi}(t) = \frac{\beta_i}{\Lambda} n_X(t) - \lambda_i C_{Xi}(t) \qquad (X,Y = A,B), \tag{2.2}$$

where $n_X(t)$=neutron population in reactor X, $C_{Xi}(t)$ = precursor population of group i=1,...,6 in reactor X, ρ_X = reactivity of the isolated reactor X, ε_{YX} = coupling coefficient for neutron exchange from Y to X≠Y. For this exchange no time lag is assumed.

For an initially critical system ($\rho_X = \rho_{Xo}$ for $t<0$) we want to compute $n_X(t)$ with $t \geq 0$ after a step change $\Delta\rho_X$ at t=0.

One easily verifies the critical condition

$$\rho_{Ao}\, \rho_{Bo} = \varepsilon_{AB}\, \varepsilon_{BA} \tag{2.3}$$

and for the ratio of neutron populations at critical

$$(n_A/n_B)_o = n_{Ao}/n_{Bo} = -\varepsilon_{BA}/\rho_{Ao} = -\rho_{Bo}/\varepsilon_{AB}. \tag{2.4}$$

In matrix form (2.1), (2.2) can be written

$$\frac{d}{dt} \vec{N}(t) = M\vec{N}(t) \tag{2.5}$$

with a column vector $\vec{N}(t)$, which has the components $n_A(t)$, $C_{A1}(t),\ldots,$ $n_B(t)$, $C_{B1}(t),\ldots,$ $C_{B6}(t)$. The constant coefficients of the matrix M can easily be constructed from (2.1), (2.2). Specific solutions of (2.5) have the form

$$\vec{N}(t) = \vec{N}_k \, e^{\omega_k t} \tag{2.6}$$

where $\vec{N}_k$ and ω_k are eigenvectors and eigenvalues obeying the eigenvalue equation

$$\omega_k \vec{N}_k = M \vec{N}_k \tag{2.7}$$

The eigenvalues ω_k are solutions of a characteristic or inhour equation, which for a system described by (2.1), (2.2) can be written |5|

$$(\omega F(\omega)-\rho_A)\,(\omega F(\omega)-\rho_B) - \varepsilon_{AB}\,\varepsilon_{BA} = 0 \tag{2.8}$$

with $$F(\omega) = \Lambda + \sum_{i=1}^{6} \frac{\beta_i}{\lambda_i+\omega}$$

As this expression is quadratic in $\omega F(\omega)$, it leads to |10|

$$\omega F(\omega) = \rho_1 \quad \text{or} \quad \omega F(\omega) = \rho_2 \quad \text{with} \tag{2.9}$$

$$\rho_{1,2} = \frac{\rho_A+\rho_B}{2} \pm \sqrt{\frac{(\rho_A-\rho_B)^2}{4} + \varepsilon_{AB}\,\varepsilon_{BA}} \tag{2.10}$$

The equations (2.9) have the form of point reactor inhour equations. Therefore, we have for each parameter, ρ_1 and ρ_2, 7 real roots, $\omega_k^{(1)}$ and $\omega_k^{(2)}$ $(k=0,\ldots,6)$, and we may split the roots of the inhour equation (2.8) for the two-point reactor accordingly. Thus, the general solution of (2.5) becomes

$$\vec{N}(t) = \sum_{k=0}^{6} a_k^{(1)} \vec{N}_k^{(1)} \, e^{\omega_k^{(1)} t} + \sum_{k=0}^{6} a_k^{(2)} \vec{N}_k^{(2)} \, e^{\omega_k^{(2)} t}. \tag{2.11}$$

Herein $\vec{N}_k^{(j)}$ $(j=1,2;\ k=0,\ldots,6)$ are the eigenvectors of (2.7) with components $n_{Ak}^{(j)}$, $C_{A1k}^{(j)},\ldots,$ $n_{Bk}^{(j)}$, $C_{B1k}^{(j)},\ldots$ The coefficients $a_k^{(j)}$ can be determined as

$$a_k^{(j)} = \left[\vec{N}_k^{(j)+} \vec{N}(o)\right] / \left[\vec{N}_k^{(j)+} \vec{N}_k^{(j)}\right] \tag{2.12}$$

where $\vec{N}_k^{(j)+}$ are the eigenvectors of the equation adjoint to (2.7) and $\vec{N}(o)$ is the state vector (2.11) for t=0. In (2.12) we exploit the fact that the two sets of eigenvectors are biorthogonal.

A significant property |10| of the eigenvectors is that in each set one can find ratios

$$\frac{n_{Ak}^{(j)}}{n_{Bk}^{(j)}} = \frac{C_{Aik}^{(j)}}{C_{Bik}^{(j)}} = \frac{\varepsilon_{BA}}{\rho_j - \rho_A} = R_j \,, \tag{2.13}$$

$$\frac{n_{Ak}^{(j)+}}{n_{Bk}^{(j)+}} = \frac{C_{Aik}^{(j)+}}{C_{Bik}^{(j)+}} = \frac{\varepsilon_{AB}}{\rho_j - \rho_A} = \frac{\varepsilon_{AB}}{\varepsilon_{BA}} R_j \tag{2.14}$$

$(i=1,\ldots,6;\ j=1,2;\ k=0,\ldots,6)$, which are independent of k. With the help of (2.8) and (2.10) we can also verify

$$R_2 = -\frac{\varepsilon_{BA}}{\varepsilon_{AB}} \cdot \frac{1}{R_1} \tag{2.15}$$

As the asymptotic behaviour of the coupled system is determined by the most positive root, called $\omega_o^{(1)}$, we deduce from (2.11) that

$$R_1 = \frac{n_{Ao}^{(1)}}{n_{Bo}^{(1)}} = \frac{n_A(t)}{n_B(t)}\bigg|_{t\to\infty} = (n_A/n_B)_\infty \,. \tag{2.16}$$

This is a measurable quantity.

To compute the $a_k^{(j)}$ from (2.12) in practice, we use the relations (2.13) to (2.16) and eliminate all precursor components using (2.2). This leads to

$$\frac{n_X(t)}{n_{Xo}} = \frac{(n_Y/n_X)_o + (n_X/n_Y)_\infty\, \varepsilon_{XY}/\varepsilon_{YX}}{(n_Y/n_X)_\infty + (n_X/n_Y)_\infty\, \varepsilon_{XY}/\varepsilon_{YX}} P(\rho_1, t) + \frac{(n_Y/n_X)_\infty - (n_Y/n_X)_o}{(n_Y/n_X)_\infty + (n_X/n_Y)_\infty\, \varepsilon_{XY}/\varepsilon_{YX}} P(\rho_2, t) \tag{2.17}$$

with $X,Y = A,B,\ X\neq Y$ and

$$P(\rho_j, t) = \sum_{k=0}^{6} \frac{1 + \frac{1}{\Lambda}\sum_{i=1}^{6} \frac{\beta_i}{\omega_k^{(j)}+\lambda_i}}{1 + \frac{1}{\Lambda}\sum_{i=1}^{6} \frac{\beta_i\,\lambda_i}{(\omega_k^{(j)}+\lambda_i)^2}} e^{\omega_k^{(j)} t} \tag{2.18}$$

$P(\rho_j, t)$ describes precisely the response of a point reactor to a step change ρ_j in reactivity starting from critical. Thus, (2.17) expresses the time behaviour of each seperate core as a sum of two terms describing point reactors.

As the root $\omega_o^{(1)}$ determines the asymptotic behaviour, we may identify ρ_1 as the reactivity of the coupled system. The term $P(\rho_2, t)$ in (2.17) contributes only, when $(n_A/n_B)_\infty \neq (n_A/n_B)_o$, i.e. if the spatial distribution of the population changes with time. ρ_2 therefore characterizes this change.

From (2.17) we get

$$P(\rho_1, t) = \frac{n_A(t)/n_{Ao}}{1+(n_B/n_A)_o\,(n_B/n_A)_\infty\,\varepsilon_{BA}/\varepsilon_{AB}} + \frac{n_B(t)/n_{Bo}}{1+(n_A/n_B)_o\,(n_A/n_B)_\infty\,\varepsilon_{AB}/\varepsilon_{BA}} \qquad (2.19)$$

Combining (2.4) and (2.13) we get also an expression for the coupling coefficient, viz.

$$\varepsilon_{XY} = \frac{\rho_1 - \Delta\rho_Y}{(n_X/n_Y)_\infty - (n_X/n_Y)_o} \,. \qquad (2.20)$$

If $\Delta\rho_Y=0$, i.e. if the reactivity is changed only in zone X, this becomes a ratio of measurable quantities.

On the other hand, (2.19) and the corresponding expression for $P(\rho_2, t)$ suggest a method to weight the time behaviour of the individual zones A and B, to isolate the terms $P(\rho_j, t)$. As these functions describe point reactors, they can be analyzed by the known methods of point reactor kinetics.

Measurements: A series of measurements were performed at the so-called two-slab loading of the Argonaut-Reactor Karlsruhe (ARK) to observe the time behaviour following step changes of reactivity. The reactor consists of a central graphite column (56.4 cm o.d.), an annular tank (92.3 cm o.d.) containing the two core zones and an outer graphite reflector. Two He^3-filled ionization chambers were placed in the outer reflector behind each zone. Their signals were amplified, converted into a pulse sequence and recorded with two synchronized 256-channel time analyzers.

Period measurements which allow to determine the reactivity ρ_1 directly were performed to derive the coupling coefficients according to eq. (2.20). The coupling turned out to be symmetrical (i.e. $\varepsilon_{AB} = \varepsilon_{BA} = \varepsilon$) within the limits of error. The coupling coefficient of $\varepsilon/\beta = 3.08 \pm 0.05$ ¢ is in good agreement with the value 3.07 ¢ obtained by a cross correlation method |11|.

Step changes of reactivity were produced by dropping one or several control and safety plates located at the interface between core and outer reflector. To demonstrate the applicability of the two-point reactor model, the results of a

measurement, where one plate at zone B was dropped, is plotted in fig. 2. Also shown is a curve, calculated on the basis of the model assuming a coupling coefficient of $\varepsilon/\beta = 3.0$ ¢ and using the reactivity change $\Delta\rho_B$ as a fitting parameter. For the best fit ($\Delta\rho_B/\beta = -1.90$ ¢) we obtained the reactivity value $\rho_1/\beta = -0.794$ ¢ with the help of eqs. (2.4) and (2.10).

To evaluate the time behaviour, a FORTRAN-programme was written which used the inverse kinetics method |12| to convert the time behaviour into reactivity values. This method is based on the point reactor model and is very sensitive against deviations from this model. The applicability to rod drop measurements has been previously shown |13|. Fig. 3 gives the results of this evaluation using (1) the data measured with each detector alone, viz. $(\rho_1/\beta)_A$ and $(\rho_1/\beta)_B$ and (2) the data weighted as given by eq. (2.19). As can be seen from fig. 3, the weighted data yield reactivity values approximately constant over the observation time. The mean reactivity value of $\rho_1/\beta = -0.801$ ¢ is in good agreement with the value obtained by the above fitting procedure.

3. Dynamic behaviour of fast reactors and excursion analysis.

In the frame of the German Fast Breeder Project the dynamic behaviour of both sodium and steam cooled fast reactors is studied. Programmes for digital and analog computers are extensively used. Only a short review of this work can be given here.

Small perturbations of steady state conditions.*) The investigation of small perturbations of a system provides information about its stability. In two digital codes |14| linearized neutron kinetics equations are used. The stability is derived from Nyquist diagrams or from Hurwitz-Routh criteria for linear systems with feedback (Doppler-, structural, can-, and coolant-coefficients). The thermodynamic analysis treats an average channel or, alternatively, the peak power channel, which may be subdivided into 30 segments.

To describe the time behaviour of numerous sodium cooled fast power reactor systems |15| a flexible analog computer programme has been established |14|. The core and total primary circuit (including the heat exchanger) can be simulated. The main non-linearities are included, so that major perturbations can be studied. For instance, flow coast down in the main coolant pumps, time delays and coolant mixing processes in the reactor inlet and outlet plenum can be simulated.

*) Investigations performed in the Institut für Reaktorentwicklung and Institut für Reaktorbauelemente.

In parallel, an analog programme has been set up for the simulation of direct cycle steam cooled fast reactors |16|. Two essential features included are: (1) Steam density is taken as temperature and pressure dependent; (2) two circuits can be treated in parallel, so that one circuit can be perturbed, the other remaining intact. Results obtained with these programmes are given in |17|.

For more accurate investigations, including super prompt critical excursions, a digital computer model is presently developed |18|. This code will use highly sophisticated equations of state for the coolant and treat several coolant channels in parallel. This will improve the averaging of the temperature across the core. The treatment of core and blanket channels with different coolant flow directions is included.

Large excursions with core disassembly. Large power excursions with subsequent disassembly of core material are analyzed using an improved Bethe-Tait model, including Doppler feedback and delayed neutrons. The originally used spherical model |19| has been abandoned, and the formalism now is applied to cylindrical cores |20|. The fundamental approximations are:

(1) One energy group. (2) Separation of neutron flux in a space-dependent shape and a time-dependent amplitude function, leading to point reactor kinetics equations. (3) Use of perturbation theory to calculate feedbacks, which is admissible only for comparatively small core density changes during the nuclear part of an excursion. As shown below, these assumptions do not hold for two-zoned fast reactor cores, with no restraints to fuel motion. If flux shape is preserved and if heat transfer can be neglected during a very fast neutronic excursion, the elevated power profile, with its discontinuity at the two-zone interface, produces a corresponding pressure step at the interface. This will induce displacement of more highly enriched material of the outer core zone into the inner zone, yielding positive reactivity. This so-called autocatalytic effect has been investigated for cylindrical cores |21|. As one important result, this autocatalytic feedback proved to be always smaller in magnitude than the negative radial disassembly feedback. Thus, an overall negative expansion feedback results in the radial direction.

In fig. 4 the time dependence of some reactivity contributions is shown for a case with a ramp reactivity insertion at 59 $/sec and a Doppler constant of $Tdk/dT = -.0035$. These parameters have been chosen as typical values for a

second excursion in the actual sodium cooled design. The excess energy, here defined as the energy stored in vaporized core material, has been calculated with and without autocatalytic effects. Results for various Doppler constants are shown in fig. 5. The rather large increases in the excursion energy release, due to the autocatalytic effect (e.g. 70% for Tdk/dT = -.004), raises the question, whether this model with its non-vanishing power-step at the interface correctly represents the physical situation.

To get a qualitative picture of the true situation at the two-zone interface, the time-dependent density ρ near this boundary has been calculated. We start from the equation of the ideal liquid ($\bar{r}$ = radial position, p = pressure obtained from the Bethe-Tait model)

$$\rho\ddot{\bar{r}} + \nabla p = 0 \qquad (3.1)$$

and the equation of continuity

$$\dot{\rho} + \nabla(\rho\dot{\bar{r}}) = 0, \qquad (3.2)$$

assuming that density changes are comparatively small before nuclear shut-down. The further assumption of a separable density function (3.3) then leads to (3.4),

$$\rho(\bar{r},t) \approx \rho_o(\bar{r}) \cdot \xi(t), \qquad (3.3)$$

$$\ddot{\xi}(t) \approx \dot{\xi}^2/\xi + \Delta p/\rho_o, \qquad (3.4)$$

$\rho_o(\bar{r})$ = initial density. For the description of the initial radial gradient in core-enrichment near the interface a continuous function like tanh $(A(r-r_z))$ is chosen, where r_z = radius of inner zone.

Calculations show that the density near the interface changes much faster than anywhere else in the core. Only 10 µsec after the begin of the disassembly we get $|\delta\rho/\rho| \approx 0.1$, a value obtained after about 4000 µsec in the core center. As one can clearly see from fig. 6, this density change at the interface immediately yields a substantial change in the power distribution, thus decreasing the power in the more highly enriched zone and increasing the power in the neighbouring zone. The observed equalization of the power near the interface, which is not taken into account in the Bethe-Tait model used, tends to reduce both the positive autocatalytic and also the negative radial expansion feedback.

It is now quite clear that in two-zone cores density changes of the core material are important for the proper description of an excursion. This has been demonstrated for the case with unrestricted radial fuel motion. Corresponding calculations show that density changes can be neglected, if only axial displacements are possible. Results for this case, given in fig. 7, show the actual density at a time, at which the density changes already have lost their influence on the development of the nuclear part of the excursion, because in this stage the energy production is almost completely due to delayed neutrons.

But, since the accidents which lead to large power excursions are in nearly all cases connected with high initial coolant temperatures*), we have to assume that the cans cannot produce radial restraint to fuel displacement. Then one must investigate properly the complicated situation at the interface between zones of different enrichment.

In order to describe reliably large power excursions in fast reactors, it is, therefore, necessary to overcome the simplifying assumptions mentioned at the beginning of this section. In addition, it is felt that strong perturbations near the zone interfaces (where normally control rods are located) will result in flux and power tilting, so that point kinetics calculations are no more applicable.

A description of the accident in every time step as quantitatively as possible then also forces us to abandon the one-group model.

The treatment of this complex space-time dynamic problem has started, using the quasistatic approximation. Another approach, not including material dislocations, uses synthesis techniques |22|. Here two-dimensional few-groups trial functions are used, which may be recalculated at several time-steps during an excursion.

The real benefit we expect from such work, for reactor designers and operators, is a better understanding of what may happen to a fast reactor. Obviously, this will have direct consequences for the layout of large fast power plants and their containment.

---

*) In those cases, where the sodium flow in most parts of the core is imperturbed during the beginning of a reactivity insertion, the cans will burst under the pressure rise within the pins and then a mixing of hot fuel and coolant with relatively low temperatures may lead to a very fast sodium vaporization.

References

|1| Uhrig, R.E. (ed.): Noise analysis in nuclear systems, AEC Symposium Series 4, TID 7679, Oak Ridge (1964),
Uhrig, R.E. (ed.): Neutron noise, waves and pulse propagation, AEC Symposium Series 9, CONF-660206, Oak Ridge (1967).

|2| Borgwaldt, H.: "Neutron Noise in a Reactor with an External Control Loop", to be published in Nukleonik (1968).

|3| Bennett, E.F.: Nuclear Sci. and Eng. 8, 53 (1960).

|4| Borgwaldt, H. and D. Stegemann: Nukleonik 7, 313 (1965).

|5| Baldwin, G.C.: Nuclear Sci. and Eng. 6, 320 (1959).

|6| Schweizer, G. and R. Lauber: Atomkernenergie 6, 242 (1961).

|7| Danofsky, R.A. and R.E. Uhrig: Nuclear Sci. and Eng. 15, 131 (1963).

|8| Seale, R.L.: Coupled core reactors, Report LAMS-2967 (1964).

|9| Köhler, W.H. et al.: Paper SM-101/51, IAEA-Symposium on Fast Reactor Physics and Related Safety Problems, Karlsruhe (1967).

|10| Kussmaul, G.: Dissertation, Karlsruhe (1968).

|11| Albrecht, R.W. and W. Seifritz: "Measurement and Analysis of the Coupled Core Coherence Function in a Two Node Symmetrical Reactor", to be published in Nukleonik (1968).

|12| Carpenter, S.G.: Nuclear Sci. and Eng. 21, 429 (1965).

|13| Kussmaul, G.: unpublished.

|14| Frisch, W. and E. Schönfeld: KFK-Report 465 (1966).

|15| Smidt, D. et al.; p. 33-45 of ANL-Report 7120 (1967).

|16| Frisch, W. and G. Woite: KFK-Report 657 (1967).

|17| Gast, K. and E.G. Schlechtendahl: KFK-Report 660 (1967),
Frisch, W. et al.: "Safety Aspects of Steam Cooled Fast Breeder Reactors", paper presented to the International Conference on Fast Reactor Safety, Aix-en-Provence, (Sept. 1967),
Erbacher, F. et al.: KFK-Report 637 (1967).

|18| Hornyik, K., private communication (1968).

|19| Braess, D. and K. Thurnay: "Theoretische Behandlung hypothetischer schwerer Unfälle bei schnellen Leistungsreaktoren", to be published in Nukleonik (1968).

|20| Braess, D. et al.: "Improvement in Second Excursion Calculations", paper presented to the International Conference on Fast Reactor Safety, Aix-en-Provence, (Sept. 1967).

|21| Braess, D. et al.: "The Calculation of Large Power Excursions Including the Autocatalytic Effect", to be published as a KFK-report (1968).

|22| Kessler, G., private communication (1968).

List of Figures

Fig. 1: Reactor with control loop and PSD measuring equipment.

Fig. 2: Ratio $n_A(t)/n_B(t)$ as a function of time t for a rod drop measurement.

Fig. 3: Reactivity as a function of time t calculated from experimental data by an inverse kinetics programme.

Fig. 4: Time behaviour of reactivities (Na2-Reactor), all disassembly effects included.

Fig. 5: Influence of autocatalytic effect on excess energies (Na2-Reactor).

Fig. 6: Density and power distribution at the zone-interface before and after the beginning of the disassembly.

Fig. 7: Density distribution in the core in a moment, in which the density change has lost its influence on the energy release of the excursion (Time: 27.16 ms). Radial displacements are suppressed.

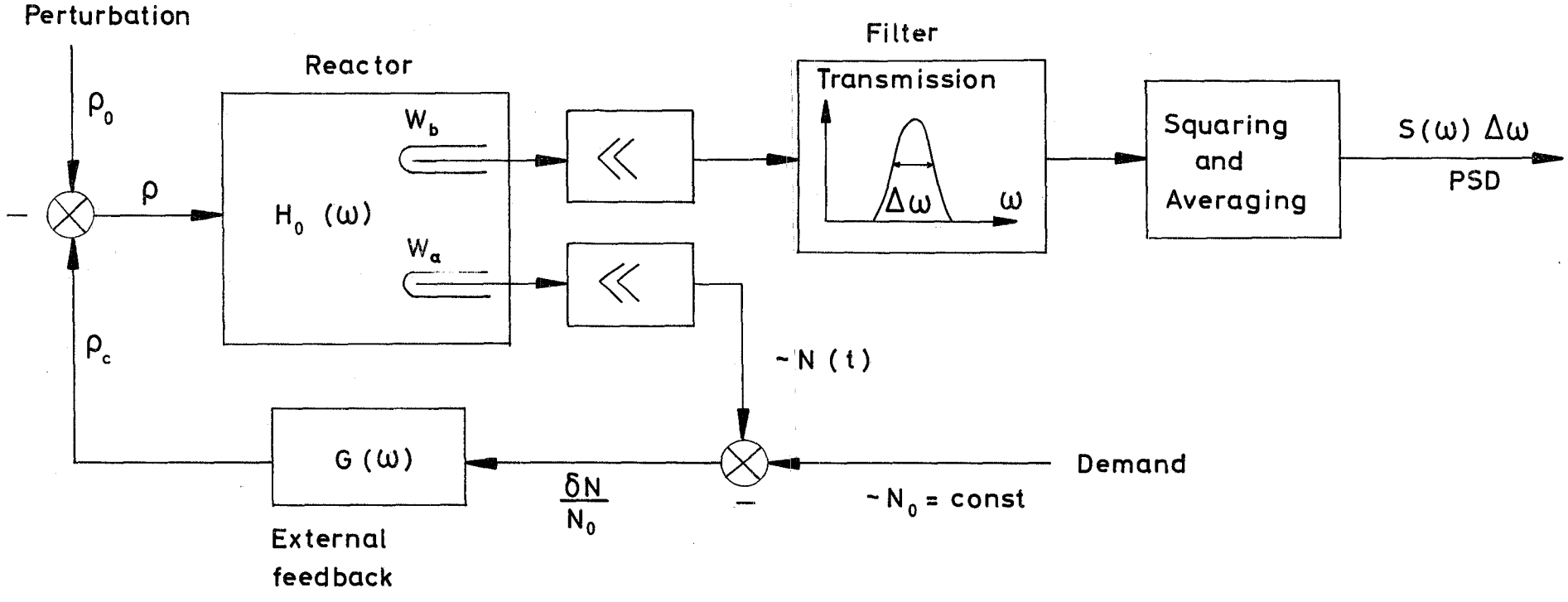

Fig. 1 Reactor with control loop and PSD measuring equipment

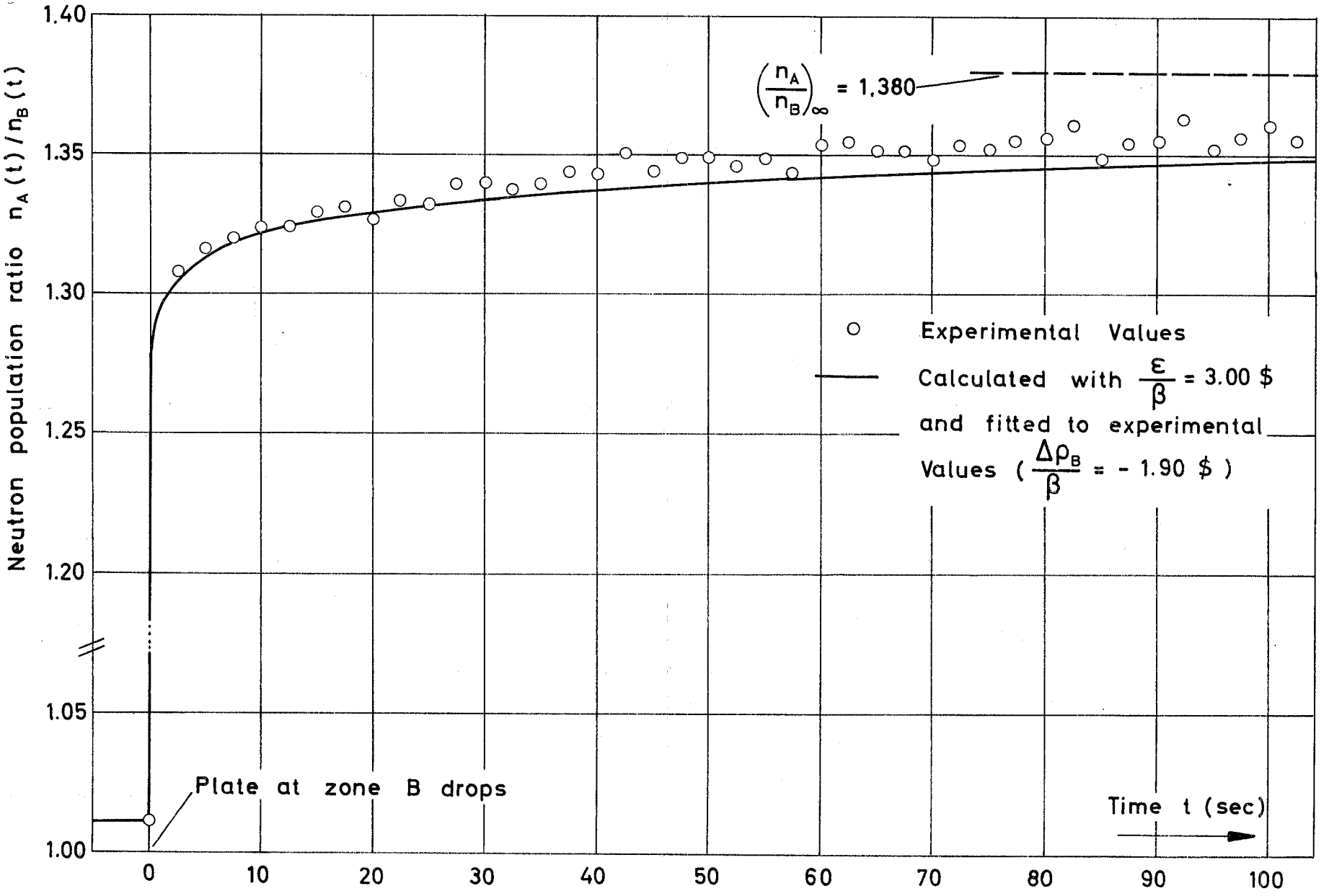

Fig. 2 Ratio $n_A(t)/n_B(t)$ as a function of time t for a rod drop measurement

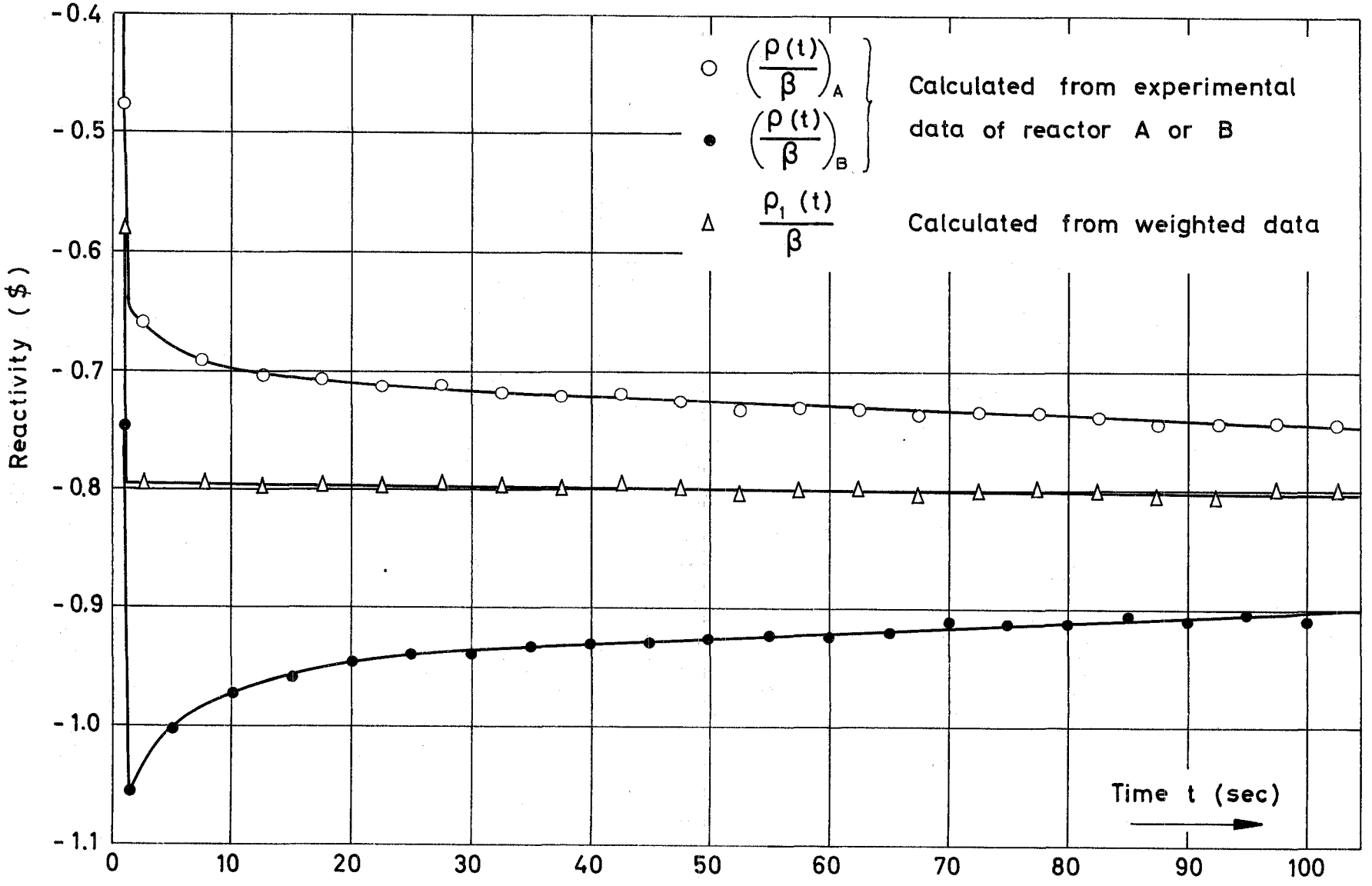

Fig. 3 Reactivity as a function of time t calculated from experimental data by an inverse kinetics programme

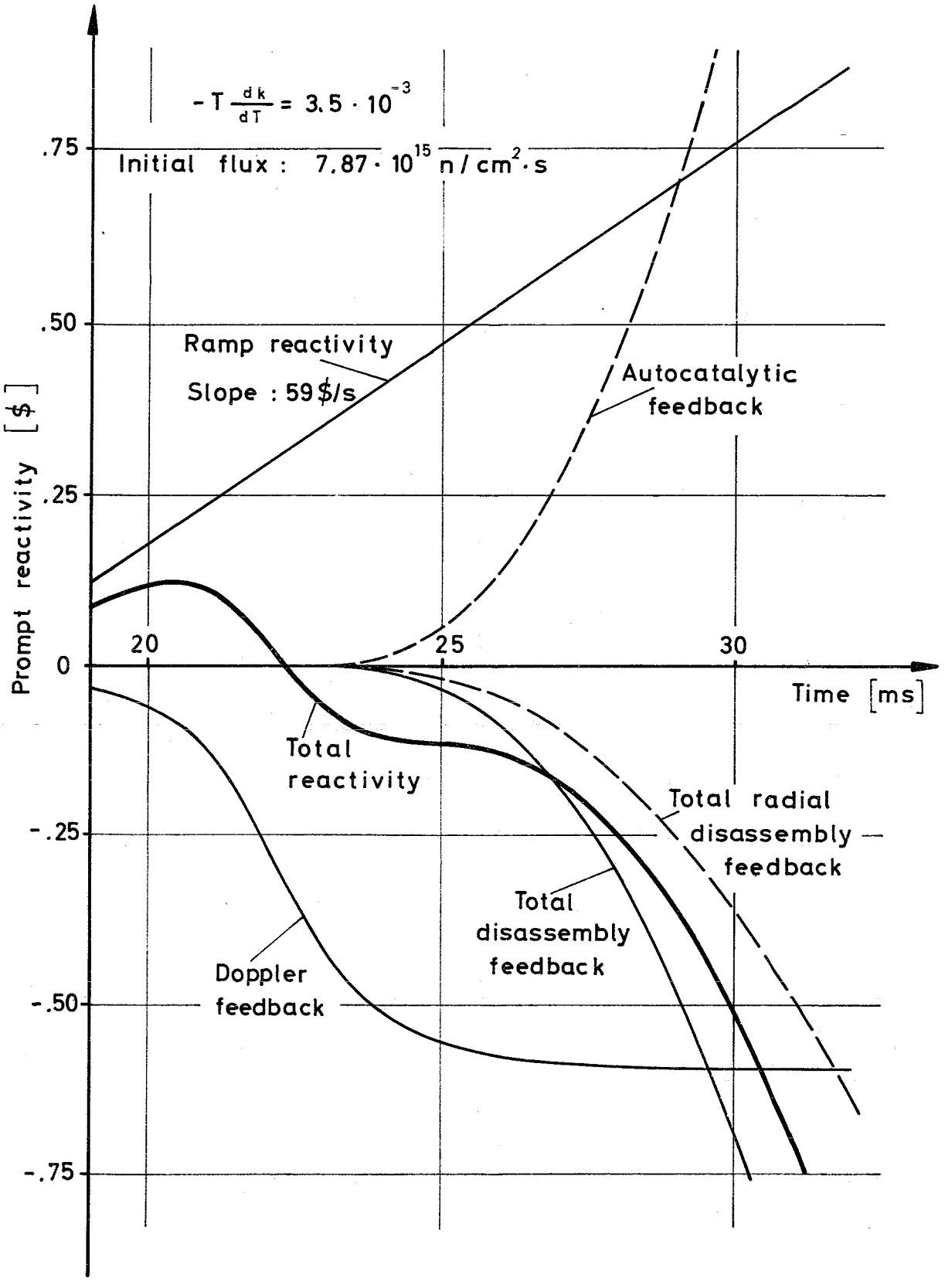

Fig. 4 Time behaviour of reactivities (Na 2 - Reactor)
All disassembly effects included

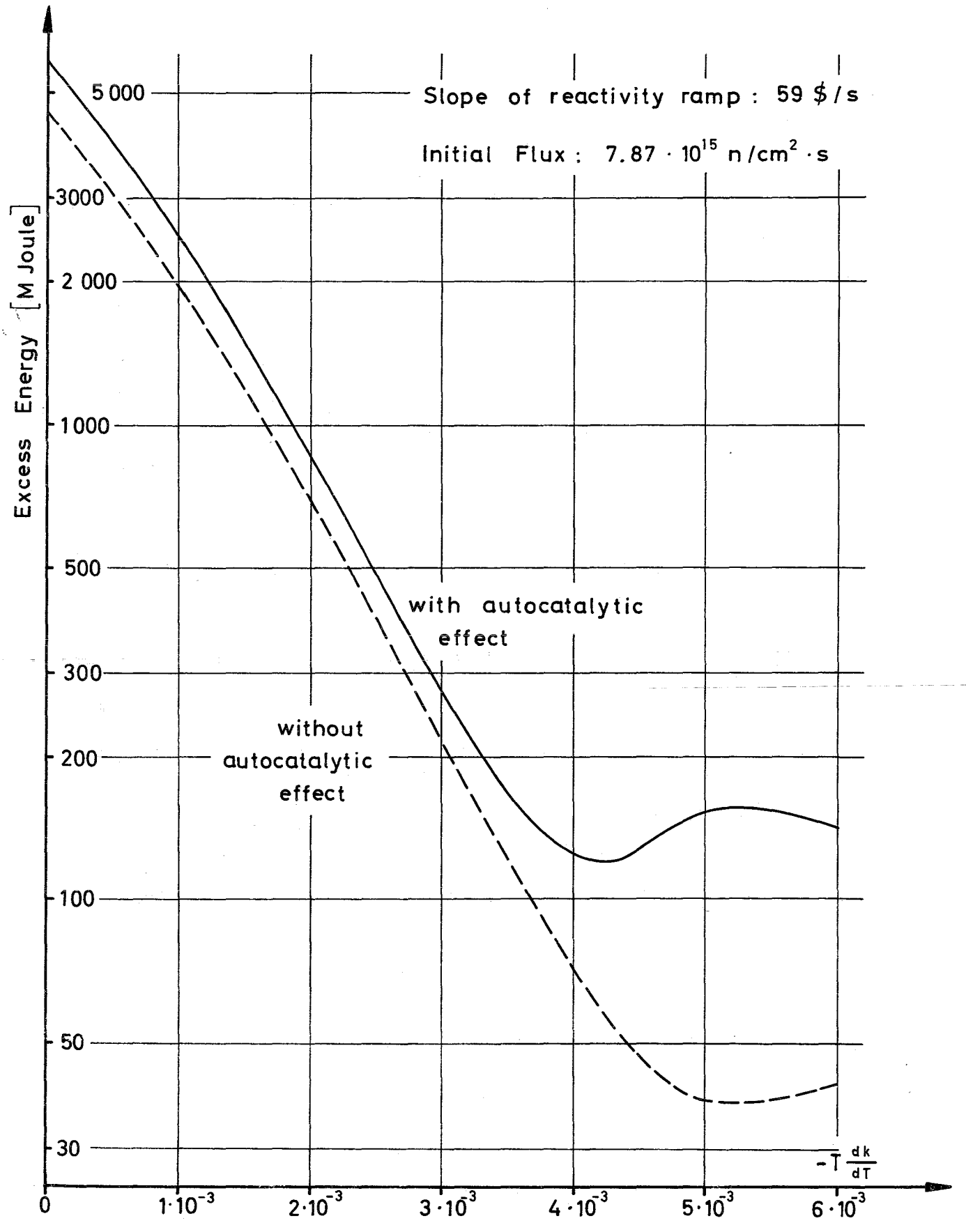

Fig. 5 Influence of autocatalytic effect on excess energies

(Na 2 - Reactor)

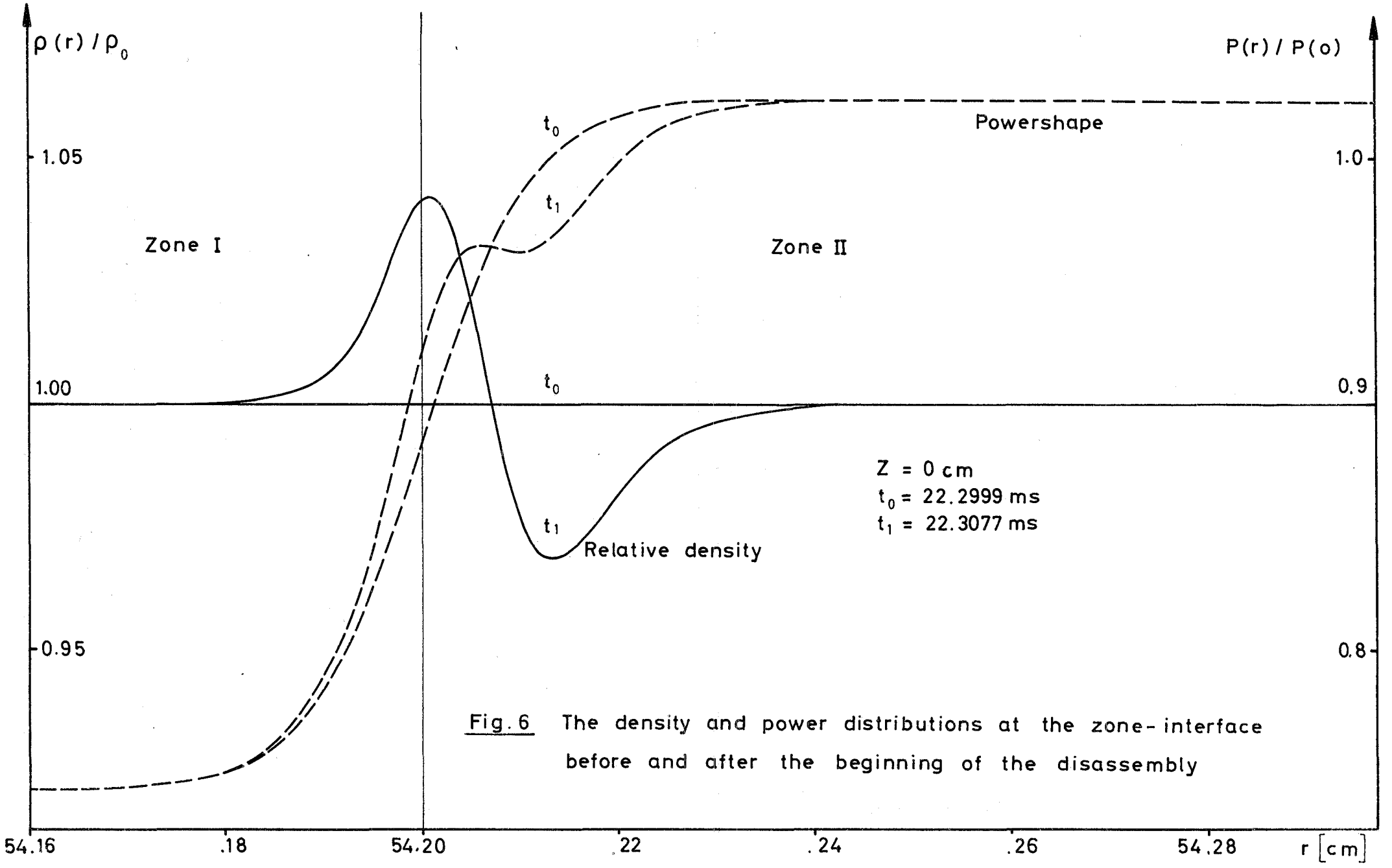

Fig. 6 The density and power distributions at the zone-interface before and after the beginning of the disassembly

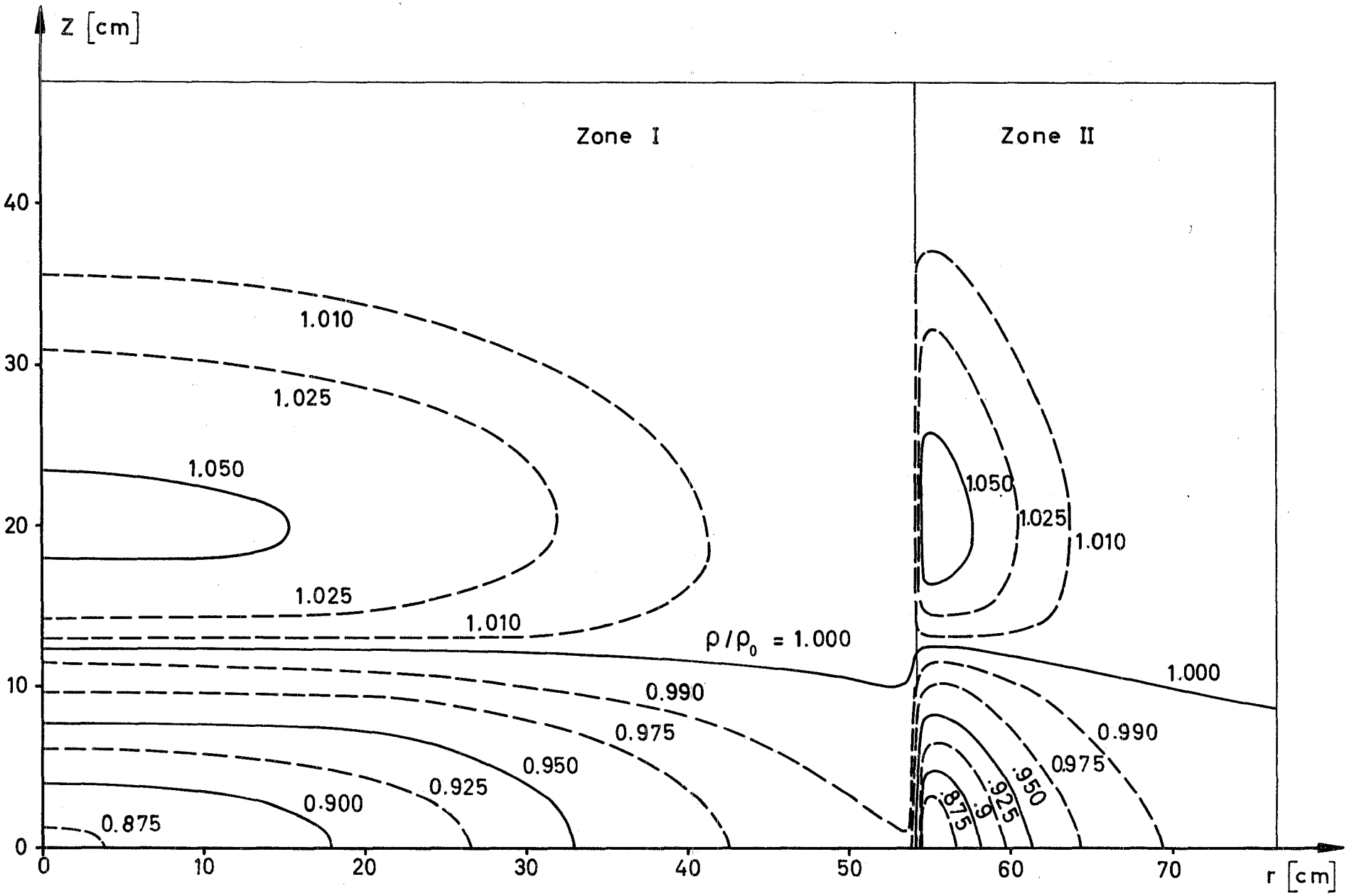

Fig. 7 Density distribution in the core in a moment, in which the density change has lost its influence on the energy release of the excursion (Time: 27.16 ms). Radial displacements are suppressed.